Dynamic Loss Minimization of Finite Control Set-Model Predictive Torque Control for Electric Drive System

Wei Xie, *Member, IEEE*, Xiaocan Wang, *Member, IEEE*, Fengxiang Wang, *Member, IEEE*, Wei Xu, *Member, IEEE*, Ralph Kennel, *Senior Member, IEEE*, and Dieter Gerling, *Member, IEEE*

***Abstract*—This paper proposes a dynamic optimization strategy of finite control set-model predictive torque control for permanent magnet synchronous machines, which takes into account the inverter losses and machine losses simultaneously. In order to reduce the switching losses (or to optimize the switching sequence) of the inverter, a recognized and feasible constrain which considers the accumulated ON/OFF times of the switches is implemented. The machine losses are taken into account by utilizing an optimal stator flux reference. An alternative loss model control method is proposed to calculate the optimal stator flux reference, which combines the conventional maximum torque/ampere method and the conventional loss model control method. Furthermore, a discrete-time machine model is introduced, which can reduce the predictive error at relative low switching frequency. The key results are illustrated by a combination of simulation and prototype interior permanent magnet machine drive measurements.**

***Index Terms*—Dynamic loss optimization, model predictive torque control, permanent magnet (PM) synchronous machines.**

I. Introduction

MODEL predictive torque control with finite control set (FCS-MPTC) is a direct torque control method. It utilizes the inherent discrete nature of the power converter. An optimization problem is solved by using a single cost function [1]–[3]. The desired voltage vector can be achieved by exhaustive exploration when the cost function is minimized. The advantages of the FCS-MPTC method are of intuitive concept and straightforward implementation [2], [4]. Furthermore, the system constraints can be easily considered by a cost function, e.g., torque performance and system losses.

Manuscript received May 19, 2014; revised December 31, 2014 and February 19, 2015; accepted February 20, 2015. Date of publication March 5, 2015; date of current version September 21, 2015. Recommended for publication by Associate Editor J. O. Ojo. *(Corresponding author: Xiaocan Wang.)*

W. Xie and D. Gerling are with the Department of Electrical Drives and Actuators, University of Federal Defense Munich, Munich 80809, Germany (e-mail: xiewei.life@gmail.com; Dieter.Gerling@unibw.de).

X. Wang and R. Kennel are with the Institute for Electrical Drive Systems and Power Electronics, Technical University of Munich, Munich 80333, Germany (e-mail: bubble88.life@gmail.com; ralph.kennel@tum.de).

F. Wang is with the Quanzhou Institute of Equipment Manufacturing, Haixi Institutes, Chinese Academy of Sciences, Jinjiang 362200, China, and also with the Institute for Electrical Drive Systems and Power Electronics, Technical University of Munich, Munich 80333, Germany (e-mail: fengxiang.wang@tum.de).

W. Xu is with Ford Motor Company, Dearborn, MI 48126 USA (e-mail: wxu29@ford.com).

Color versions of one or more of the figures in this paper are available online at http://ieeexplore.ieee.org.

Digital Object Identifier 10.1109/TPEL.2015.2410427

The application of FCS-MPTC method for inverters has been investigated and analyzed [5]. The FCS-MPTC method can take into account the usual control objectives presented in the traditional applications and the extra targets. The extra constraints can include the balance of the reduction of switching losses, the effective switching frequency, the power losses, and the dc-link voltage. In [6], the limit of the switching frequency of the three-level neutral-point-clamped converter is considered by a cost function. One term n_c is defined, which is proportional to the number of commutations of the power semiconductors between two sampling steps. A neutral-leg switching frequency reduction algorithm is proposed to improve the efficiency of the two-level four-leg inverters [7], [8], which takes into account the switching loss by extra constraints in the cost function. The balanced loss distribution of normal two-level voltage source inverter (VSI) of FCS-MPTC has been analyzed in [9], which proposes a switching strategy to optimize the clamped phase among the three legs and focuses on the inverter loss. Based on the preceding investigation, the conventional constraints of the power semiconductors [6] are applied in this paper.

Concerning the wide application of electrical motor drive systems, e.g., over half of the electrical energy produced worldwide is used by motors [10], until now, significant efforts and attentions are given to improve the system efficiency. The system efficiency due to the machine design can be improved by a novel topology [11], [12]. The system efficiency which depends on the modern control methods (e.g., FCS-MPTC method) can be improved by optimizing the control methods. At relative low speed, as long as the copper losses are dominant, the maximum torque per ampere (MTPA) strategy is an option to the efficiency optimization [13]–[15]. The loss-minimizing control (LMC) methods in electrical drive systems have been investigated for over 30 years, which can take into account the system losses. The existing methods can be divided into two groups: model-based steady-state methods [16], [17], and physical-based searching control (SC) methods [18], [19].

The principle of model-based LMC methods for interior permanent magnet synchronous machines (IPMSMs) is that the equivalent iron loss and permanent magnet (PM) resistances are integrated into the equivalent circuit of the IPMSMs, and then the optimal d-axis current can be obtained when the copper loss, iron loss, and PM loss are minimized. In order to improve the accuracy of the iron loss model, finite-element method (FEM) and experimental loss measurement methods are proposed by taking the saturation effect into account [20]. One drawback of

the model-based LMC is that only the steady-state machine loss is modeled and optimized, while the inverter loss optimization is ignored. The physical-based SC methods depend neither on the motor model nor on the motor parameters. It measures and minimizes the input power (dc bus power) by iterating the reference of d-axis current or the stator flux reference [19], [21]. The main advantages of the physical-based SC methods are the independence of the system parameters (e.g., machine and inverter parameters) and optimization of the whole system. However, the slow real-time convergence of these methods is induced by the exhaustive exploration. Thus, the physical-based SC methods are not the preferable strategies for electric drives with fast dynamic response.

The widely accepted MTPA method and LMC method are attracting growing attention for efficient optimal application. The principle is that the methods utilize an adapting control variable (e.g., d-axis current or stator flux reference) to improve the efficiency. For LMC algorithm, both of copper loss, iron loss and PM loss can be considered and optimized. It is quite intuitive that the loss model is more precise, and the LMC implementation is more effective [16]. From another standpoint, the approach of LMC may fail if the loss model is not accurate enough. Another overview of the LMC methods is that when the number of the constraints increases, a relative low convergence speed is induced.

In this paper, an alternative LMC method which is combining a conventional MTPA method with a conventional LMC method is proposed. The machine losses are minimized by commanding optimal stator flux magnitude. At low speed, MTPA trajectory is chosen, while at medium and high speed, the LMC trajectory dominates. Meanwhile, the optimization of the dynamic switching sequence of the switches of the inverter is applied, which can reduce the switching losses of the inverter indirectly.

At this moment, the existing high sampling frequency and high switching frequency of FCS-MPTC strategies are formed using approximate discrete-time modeling technique, which assumes the sampling frequency and switching frequency are high enough to ignore the approximation error. However, in particular for high-power traction drive applications as medium large traction drive, the switching frequency is constrained to a relative low value because of the high temperature caused by the high switching loss due to the high switching frequency. Furthermore, in long-horizon prediction FCS-MPTC method, the switching frequency is limited to a low value because of the computation delay. In this case, the torque and current estimation error for the FCS-MPTC strategies due to the approximate discrete-time modeling technique will become serious. Thus, this paper proposes an alternative discrete machine model based on the modified Euler method (trapezoidal method).

This paper is organized as follows: Section II introduces the loss model of the inverter and the IPMSMs. In Section III, the proposed LMC method is explained. Section IV introduces the alternative discrete-time machine model and the implementation of the FCS-MPTC with the proposed LMC method. The experimental results are investigated and analyzed in Section V. Finally, this paper is concluded in Section VI.

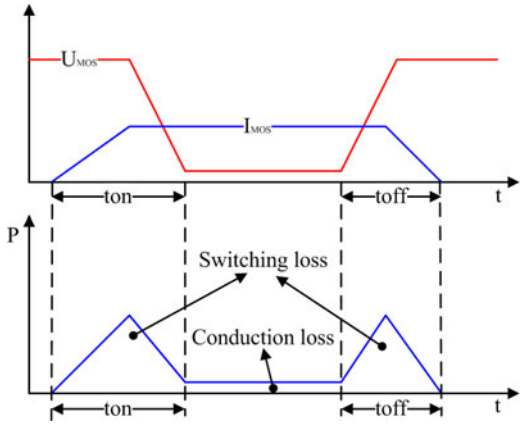

Fig. 1. Switching transients of the power MOSFET [22].

II. Loss Model

A. Loss Model of Inverter

The losses of the power semiconductors (e.g., MOSFET) can be divided into the switching loss and the conduction loss. The switching loss rise significantly with the increase of switching frequency. Similar to the switching loss, the conduction loss also depends on the applied voltage and the phase current, as shown in Fig. 1 [22]. The phase current depends only on the operating point given by the torque and the speed, but not on the switching pattern. Hence, the conduction losses can be considered to be independent from the switching pattern. In [23], the switching loss is described as follows:

$$P_{\text{sw-loss}} = \left(\frac{A}{2} + \frac{BI_{\text{rms}}}{\pi} + \frac{CI_{\text{rms}}^2}{4}\right)\frac{U_{\text{dc}}}{U_{\text{data}}} f_{\text{sw}} \tag{1}$$

where, A, B, and C are the polynomial coefficients of switching energy, I_{rms} is the current flowing through the switch, U_{data} is the voltage corresponding to the energy curves, and f_{sw} is the switching frequency.

From Fig. 1 and (1), it can be seen that the switching loss of the inverter is directly proportional to the switching frequency. It means that the lower ON/OFF times of the switch represent the lower switching loss. Thus, one of the key points of the inverter loss optimization is to minimize the ON/OFF times by switching sequence optimization. When the long-horizon prediction of model predictive control is set as 2, the switching sequence can be optimized between two sampling periods.

B. Loss Model of IPMSMs

By taking into account the copper loss, iron loss, and PM loss, an equivalent circuit with series-parallel structure is introduced, as shown in Fig. 2, where, R_{Fe} and R_{PM} are the equivalent iron loss and PM loss resistances, respectively, which are achieved based on FEM results indirectly; and i_{Loss} is the equivalent iron loss and PM loss current. Based on the equivalent circuit Fig. 2,

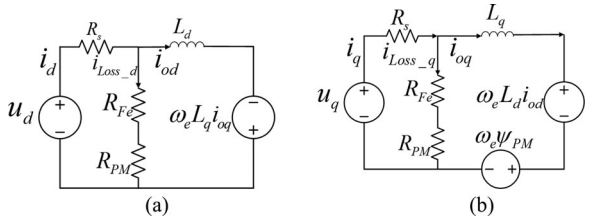

Fig. 2. Equivalent circuit of IPMSM in dq reference frame including loss. (a) Equivalent circuit of d-axis. (b) Equivalent circuit of q-axis.

the copper loss, iron loss, and PM loss can be described as

$$P_{\text{cu}} = \frac{3}{2}R_s \left[\left(\frac{\psi_d - \psi_{\text{PM}}}{L_d}\right)^2 + \left(\frac{T_e}{\frac{3}{2}p[\frac{\psi_{\text{PM}}}{L_q} + (L_d - L_q)\frac{\psi_d - \psi_{\text{PM}}}{L_d L_q}]}\right)^2\right] \quad (2)$$

$$P_{\text{Fe}} + P_{\text{PM}} = \frac{3}{2}\frac{\omega_e^2}{R_{\text{Fe}} + R_{\text{PM}}}(\psi_q^2 + \psi_d^2). \quad (3)$$

III. Proposed LMC Method

A. Conventional MTPA Method

The MTPA method, developed by Jahns *et al.* [13], is a current minimizing solution, which is used to reduce the size of the inverter. The MTPA method can minimize the copper loss by optimizing the d- and q-axis current. At relative low speed, the iron loss and PM loss are not dominant of the machine losses. Thus, the MTPA strategy is an option for the partial efficiency optimization. The MTPA operating point is the nearest point to the peak value of the torque. Therefore, in the synchronous reference frame, the differentiation of the torque with respect to the load angle ($\partial T_e/\partial\delta$) should be zero at the MTPA point. The solution of load angle of MTPA method can be calculated by [24]

$$\delta_{\text{MTPA}} = \cos^{-1}\left(\frac{-\psi_{\text{PM}} + \psi_{\text{PM}}^2 + 8(L_d - L_q)^2|\mathbf{i}_s^2|}{4(L_d - L_q)|\mathbf{i}_s|}\right). \quad (4)$$

Then, the d- and q-axis currents reference can be described as

$$i_{d-\text{MTPA}} = \mathbf{i}_s \cos(\delta_{\text{MTPA}}) \quad (5)$$

$$i_{q-\text{MTPA}} = \mathbf{i}_s \sin(\delta_{\text{MTPA}}). \quad (6)$$

When the copper loss is described through the stator flux, it is shown in (2). The stator flux reference which can achieve the minimum copper loss can be calculated through $\partial(P_{\text{cu}})/\partial(\psi_s) = 0$. In order to simplify the solution, using curve fitting method, the optimal stator flux of MTPA in this paper is expressed as

$$\frac{\psi_{s-\text{MTPA}}}{\text{V}\cdot\text{s}} = 0.0000735\left(\frac{T_e}{\text{N}\cdot\text{m}}\right)^2 + 0.0000596\left(\frac{T_e}{\text{N}\cdot\text{m}}\right) + 0.00704. \quad (7)$$

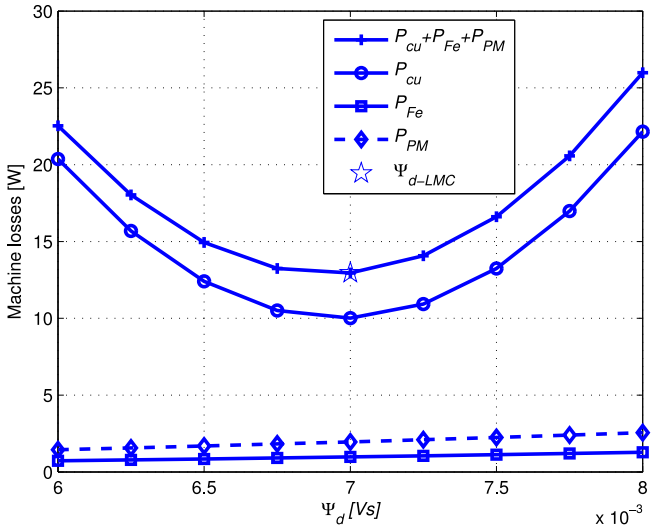

Fig. 3. Copper loss, iron loss, and PM loss based on d-axis flux.

B. Conventional LMC Method

The machine losses have been described as (2) and (3). Omitting the tedious derivation process, it can be proved that the total machine losses are a convex function of ψ_d, as

$$\frac{\partial^2(P_{\text{Fe}} + P_{\text{PM}} + P_{\text{cu}})}{\partial(\psi_d)^2} > 0 \quad (8)$$

$$\frac{\partial(P_{\text{Fe}} + P_{\text{PM}} + P_{\text{cu}})}{\partial(\psi_d)} = 0. \quad (9)$$

The losses corresponding to ψ_d at constant speed are shown in Fig. 3. It can be seen that the optimal flux point $\Psi_{d-\text{LMC}}$ corresponds to the minimum machine losses. Therefore, the solution procedure of optimal stator flux is a process of resolving the order ordinary differential equation (ODE), as (9). Omitting the tedious derivation process, the solution of stator flux is expressed as (10). The coefficients of (10) can be calculated by Ferraris solution, as shown in Appendix A

$$\psi_{d-\text{LMC}} = \frac{-b_1}{4a_1} + \frac{-\sqrt{B_1 + 2y - \sqrt{-(3B_1 + 2y - \frac{2B_2}{\sqrt{B_1+2y}})}}}{2}. \quad (10)$$

C. Proposed LMC Method

The accuracy of the estimated rotor losses is mainly determined by the accuracy of the employed device and the involved test environment [25], [26]. Even with the accurate and complex experimental measurements, due to the small percentage of iron loss and PM loss compared with total machine losses at relative low speed, it is still a challenge to keep the accuracy of the iron loss. The disadvantage of the MTPA method is that it directly ignores the iron loss and PM loss. Therefore, it is desirable to design a control method that is less sensitive to the measurement of accuracy of iron loss and PM loss at relative low

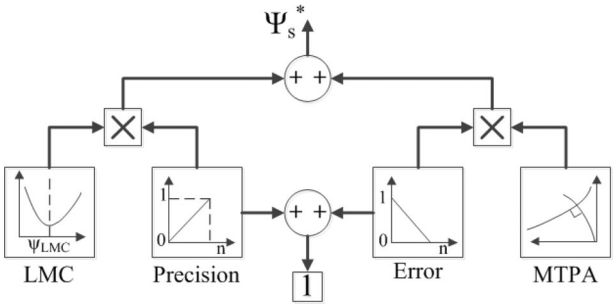

Fig. 4. Scheme of the Gopinath-style LMC method.

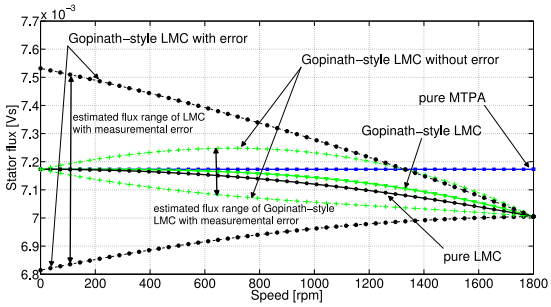

Fig. 5. Trajectory of the stator flux reference of the Gopinath-style LMC method.

speed. This method should take the copper losses, iron losses, and PM losses into account at relative high speed. In this paper, a proposed LMC method is developed by combining the pure MTPA method and the conventional LMC method. In order to understand this method easily, it is named as the Gopinath-style LMC method. In the proposed Gopinath-style loss minimizing method (LMC), a function of measurement error of iron loss and PM loss is built as (11). The error function has the same function of bandwidth in Gopinath-style flux observer [27], which produces a smooth transition between the MTPA solution and the LMC method. The scheme of the proposed Gopinath-style LMC method is shown in Fig. 4. Fig. 5 shows the trajectory and the error range of the estimated stator flux reference. The trajectories of the "pure MTPA method" and the "LMC method" are achieved by assuming that the measurement error of the iron loss and PM loss is zero. The two lines named as "pure LMC with error" build the range of the flux trajectory of pure LMC with measurement error. The two lines (Gopinath-style LMC with error) represent the top margin and bottom margin of the trajectory of the Gopinath-style LMC method, which take into account the measurement error of the iron loss and PM loss. It can be seen that as compared with the pure LMC method, the alternative Gopinath-style LMC method reduces the error area of the stator flux reference significantly

$$E_{\text{iron}} = 1 - \frac{1}{\omega_b}\omega. \tag{11}$$

As a graphical summary, Fig. 6 shows the current trajectory of the MTPA method ($\overline{OA}$) and the LMC method ($\overline{OB}$) on a dq coordinate system.

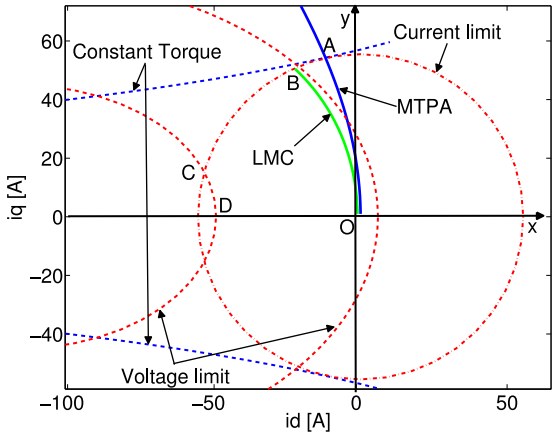

Fig. 6. Trajectory of MTPA and LMC.

IV. Proposed FCS-MPTC With Efficiency Optimization

A. Discrete Model of IPMSMs

For the IPMSMs, the relations between the flux, current, speed, and electromagnetic torque can be described as the following ODEs (12)–(14) [3], [28]:

$$\frac{d\mathbf{i}_s}{dt} = \mathbf{L}_s^{-1}(\mathbf{u}_s - R_s\mathbf{i}_s - \frac{\partial \mathbf{L}_s}{\partial\theta} - j\omega\mathbf{\Psi}_{\text{PM}}) \tag{12}$$

$$\frac{d\omega}{dt} = \frac{p}{J}(T_e - T_L) \tag{13}$$

$$\frac{d\theta}{dt} = \omega. \tag{14}$$

Internal discrete-time model of the electric drive is necessary, which is used to predict the future evolution of the controlled output variables for a sequence of control inputs over a prediction horizon (one sampling period T_s). The conventional FCS-MPTC is based on the forward Euler method to predict the flux and electromagnetic torque in the electric drives, and the forward Euler discretization is shown as (15) [3]. In order to improve the accuracy of the discrete machine model, this paper proposed an alternative machine model based on the modified Euler method (trapezoidal method), as described in (16)

$$y(k+1) = y(k) + T_s f(k, y(k)) \tag{15}$$

$$\begin{cases} \overline{y(k+1)} = y(k) + T_s f(k, y(k)) \\ y(k+1) = y(k) + \frac{T_s}{2}[f(k, y(k)) \\ \qquad\qquad + f((k+1), \overline{y(k+1)})]. \end{cases} \tag{16}$$

Omitting the tedious derivation, an alternative discrete current function of IPMSMs can be described as (17). The coefficient matrices are expressed in (18)–(20)

$$\hat{\mathbf{i}}_s(k+1) = A\mathbf{i}_s(k) + B\mathbf{u}_s(k) + C \tag{17}$$

where (18) – (20) as shown bottom of the next page.

Based on the simulation results of partial load step, the proposed model for IPMSMs is evaluated and compared with the existing conventional frequency model. The traditional and

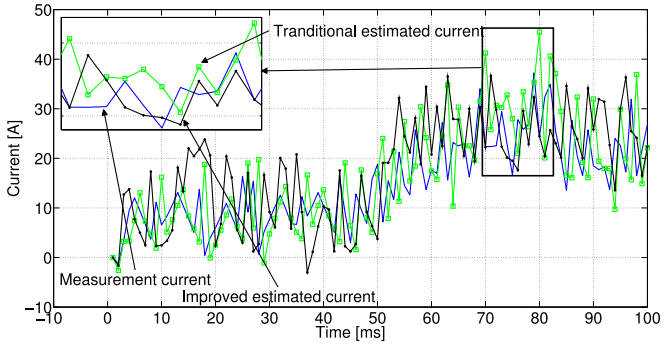

Fig. 7. Comparison between current prediction strategies with 2-kHz switching frequency.

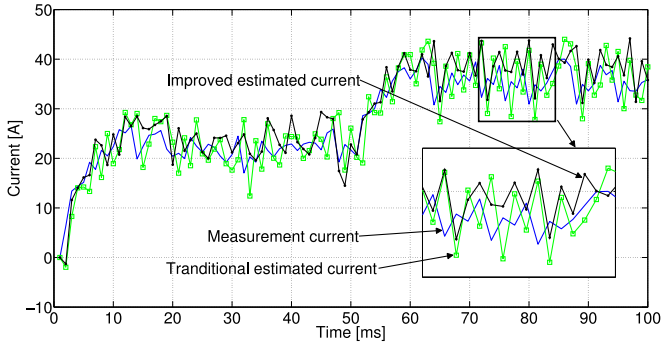

Fig. 8. Comparison between current prediction strategies with 5-kHz switching frequency.

improved estimated current, which are based on the existing standard model and the proposed low-frequency model, respectively, are plotted and overlaid with the actual measurement current for comparison. The traditional estimated current and the improved estimated current are achieved by the conventional machine model and the proposed machine model, respectively, which represent the predictive current at future step (e.g., $(k+1)$th sampling period). From Fig. 9, it can be seen that when the switching frequency is high enough (e.g., 10 kHz), the estimated current and measurement current are overlapped with each other. It verifies that the approximate discrete-time modeling technique can provide accurate dynamic stator current prediction at relative high-frequency operation. As shown in Figs. 7 and 8, at relative low switching frequency, compared with the traditional model, the current estimated by the proposed discrete machine model can track the actual current with lower oscillation. It can be concluded that as compared with the conventional high-frequency model, the proposed low-frequency model somehow compensates the predictive error.

Then, based on the machine model and predicted stator current, the stator flux and electromagnetic torque at $(k+1)$th sampling period can be predicted through

$$\hat{\boldsymbol{\Psi}}_s(k+1) = \boldsymbol{\Psi}_s(k) + (\mathbf{u}_s(k) - R_s\mathbf{i}_s(k))T_s \tag{21}$$

$$\hat{T}_e(k+1) = \frac{3}{2}p\hat{\boldsymbol{\Psi}}_s(k+1)\hat{\mathbf{i}}_s(k+1). \tag{22}$$

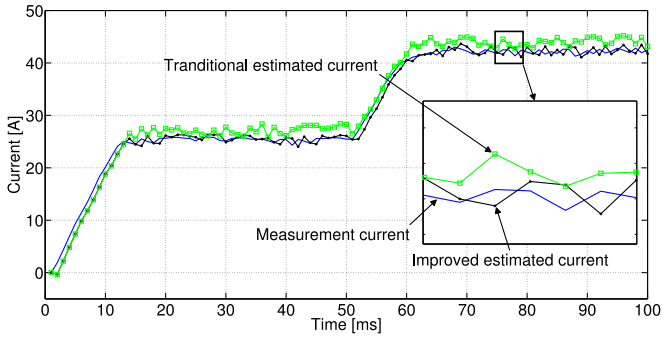

Fig. 9. Comparison between current prediction strategies with 10-kHz switching frequency.

B. Cost Function and Control Scheme

The cost function of the proposed FCS-MPTC method is the criterion to select the best voltage vector among the feasible ones. Here, the traditional two-level VSI is used. The cost function of this paper is expressed as

$$\begin{aligned} g_i = \frac{1}{2}\sum_{n=1}^{N}\{&|T_e^*(k) - \hat{T}_e(k+n)_i|^2 \\ &+ Q_1||\boldsymbol{\Psi}_s(k)|^* - |\hat{\boldsymbol{\Psi}}_s(k+n)_i||^2 \\ &+ Q_2|S(k) - S(k+n)_i|^2\} + I_{\max} \end{aligned} \tag{23}$$

$$A = \begin{bmatrix} 1 + \frac{T_s}{2}\left[\left(1 - \frac{R_sT_s}{L_d}\right) + a\left(\left(1 - \frac{R_sT_s}{L_d}\right)^2 - (T_s\omega_e(k))^2\right)\right] & \frac{T_s}{2}\left[\frac{L_qT_s\omega_e(k)}{L_d} + a\left(\frac{L_qT_s\omega_e(k)}{L_d}\left(2 - \frac{R_sT_s}{L_d} - \frac{R_sT_s}{L_q}\right)\right)\right] \\ \frac{T_s}{2}\left[\left(-\frac{L_dT_s\omega_e(k)}{L_q}\right) + b\left(\frac{L_dT_s\omega_e(k)}{L_q}\right)\left(2 - \frac{R_sT_s}{L_d} - \frac{R_sT_s}{L_q}\right)\right] & 1 + \frac{T_s}{2}\left[\left(1 - \frac{R_sT_s}{L_q}\right) + b\left(1 - \frac{R_sT_s}{L_q}\right)^2 + (T_s\omega_e(k))^2\right] \end{bmatrix} \tag{18}$$

$$B = \begin{bmatrix} \frac{T_s}{2}\left[\frac{T_s}{L_d} + a\left(\frac{T_s}{L_d}\left(2 + \frac{R_sT_s}{L_d}\right)\right)\right] & 0 \\ -b\frac{T_s^3}{2}\left(\frac{\omega_e(k)}{L_q}\right)\frac{T_s}{2}\left(\frac{T_s}{L_q} + b\left(\frac{T_s}{L_q}\left(2 + \frac{R_sT_s}{L_q}\right)\right)\right) & \end{bmatrix} \tag{19}$$

$$C = \begin{bmatrix} \frac{a(T_s\omega_e(k))^2\psi_{\mathrm{PM}}}{2L_d} \\ -\frac{T_s}{2}\left[-\frac{T_s\psi_{\mathrm{PM}}\omega_e(k)}{L_q} + b\left(\frac{T_s\psi_{\mathrm{PM}}\omega_e(k)}{L_q}\right)\left(2 - \frac{R_sT_s}{L_q}\right)\right] \end{bmatrix} \tag{20}$$

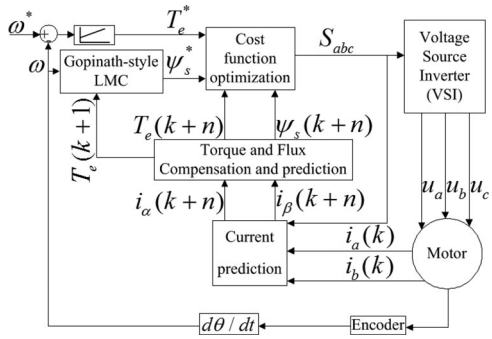

Fig. 10. Block diagram of FCS-MPTC with loss optimization.

where $i = 1, \ldots, 7$ is the available numbers of the voltage vector of the two-level inverter; g_i is the cost value due to the voltage vector i of $(k+n)$th sampling time; and $T_e^*(k)$ and $|\boldsymbol{\Psi}_s(k)|^*$ are the reference torque and the reference amplitude for the stator flux at (k)th sampling time, respectively. $\hat{T}_e(k+n)$ and $|\hat{\boldsymbol{\Psi}}_s(k+n)|$ are the predicted electric torque and the amplitude of the predicted stator flux for a given switching state due to voltage vector i at $(k+n)$th sampling period, respectively. $S(k)$ means the number of commutations of the power semiconductors between (k)th and $(k-1)$th sampling period. The weighting factor Q_1 is used to adjust the importance of the flux error with respect to the torque error. Q_2 is the weighting factor that determines the importance of machine loss and inverter loss compared to the torque control. The weighting factors are calculated based on the iterative evaluation method [29]. In this paper, in order to achieve the dynamic losses optimization, at each period, the average torque, flux, and switching numbers will be recalculated and achieved by the unitary method, as seen in Appendix B. As a protection, the current limitation term is important, it is defined as (24).

The proposed Gopinath-style LMC method is integrated into traditional FCS-MPTC to achieve the optimal reference of stator flux. Furthermore, in the cost function, by taking the switching sequence of the inverter into account, the balance between machine losses and inverter losses can be considered. The control scheme of the proposed FCS-MPTC with the Gopinath-style LMC method is shown in Fig. 10

$$I_{\max} = \begin{cases} 0, & if |i(k+n)| \le |i_{\max}| \\ \infty & if |i(k+n)| > |i_{\max}|. \end{cases} \tag{24}$$

V. Experiment Evaluation

The proposed FCS-MPTC with the Gopinath-style LMC method is tested and compared experimentally to the conventional FCS-MPTC strategy for a IPMSM. The machine parameters are summarized in Table. I. In order to evaluate the validity of the proposed strategy, both of the FCS-MPTC with the Gopinath-style LMC method (hereafter referred to as MPTC-LMC method for a simple description) and the conventional FCS-MPTC (hereafter referred to as MPTC) will be based on the same speed PI controller ($K_p = 0.219$ and $K_i = 0.16$) and same predictive step ($N = 2$). Their performances are shown and analyzed in this section. The IPMSM is driven by a modified 2-kV·A inverter, which provides full control over the MOSFET gates, and the maximum switching frequency of the inverter is 50 kHz. The dSPACE control platform has the ability to perform 2500 million instructions per second. In this experiment, the turnaround time is about 90 μs, which includes the communication time between dSPACE and control desk, the A/D and D/A conversion time, the code implementation time, and the data saving time. Thus, the sampling cycle of the control system is set as 100 μs, which means the sampling frequency is 10 kHz. The overview of the test bench is shown in Fig. 11.

TABLE I
Parameters of the Tested IPMSM

Rated torque	2 N·m
Rated current/voltage (rms)	50 A/8.5 V
Number of Pole pair	5
d/q-axis inductance	0.05/0.095 mH
Resistance	18 mΩ
Flux linkage of PM	7.07 mV·s
Rated/maximum speed	2000/4000 r/min
The moment of inertia	0.00187 Kg/m^2

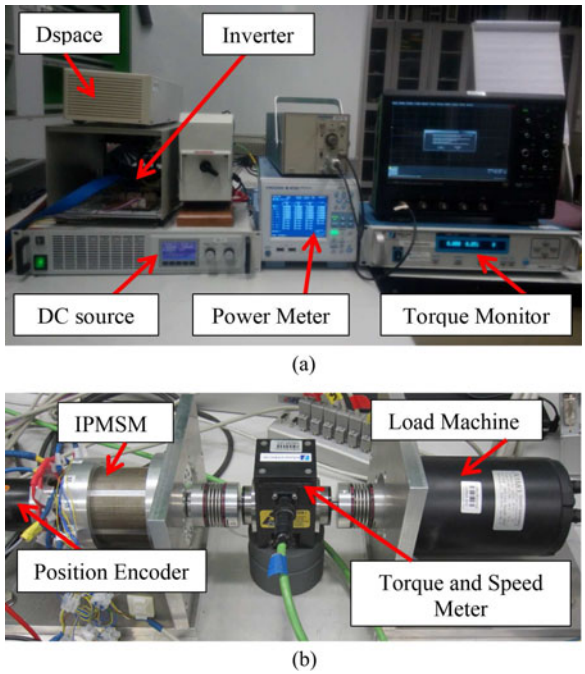

Fig. 11. Test bench. (a) Control interface. (b) Test machine and load machine.

A. Steady-State Performance

This section shows the validity of the proposed MPTC-LMC method at steady state. The experimental results are obtained with the 2 N·m (1 $p.u$) load torque at $n = 2000\ r/\text{min}$ (1 $p.u$). The comparisons of torque and current between the MPTC-LMC method and the MPTC method are shown in Figs. 12 and 13. It can be seen that the torque and current performance of the MPTC-LMC method are similar to that of the MPTC

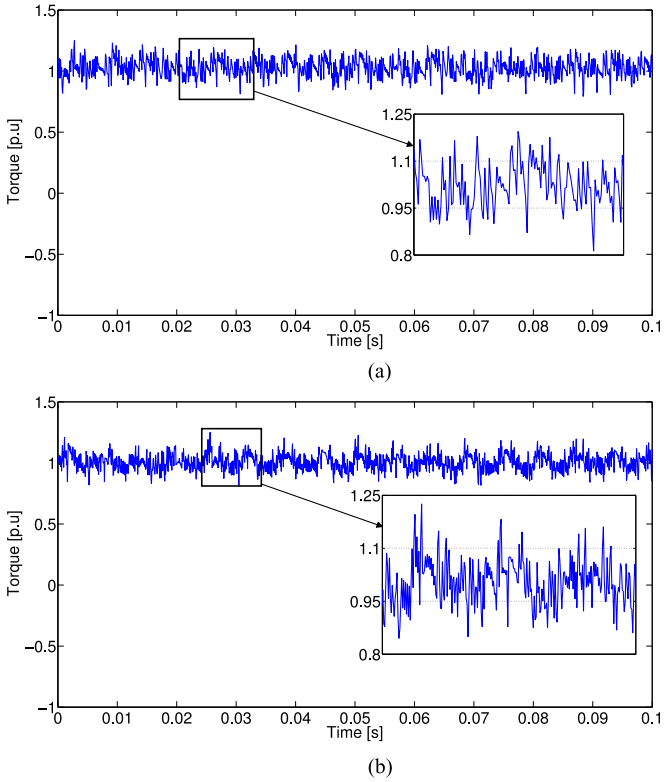

Fig. 12. Steady-state torque. (a) MPTC-LMC. (b) MPTC.

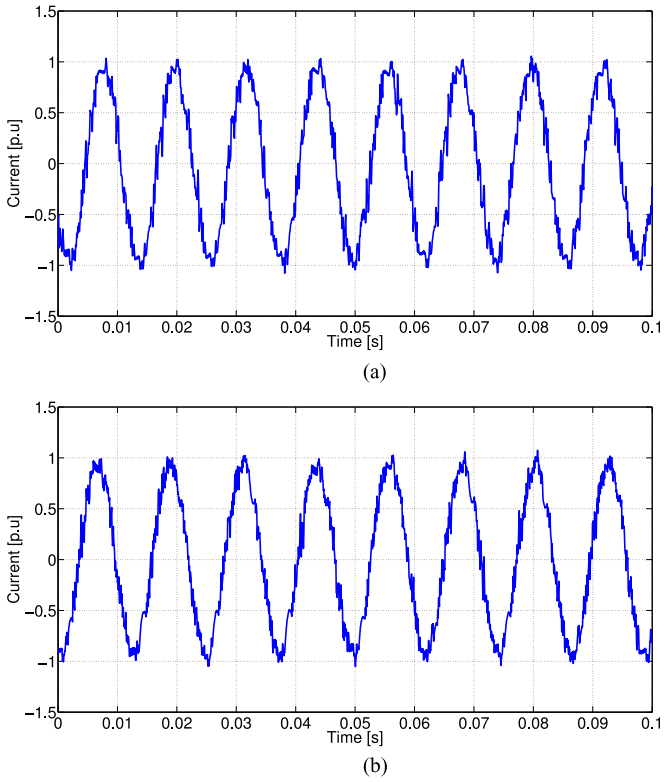

Fig. 13. Steady-state current. (a) MPTC-LMC. (b) MPTC.

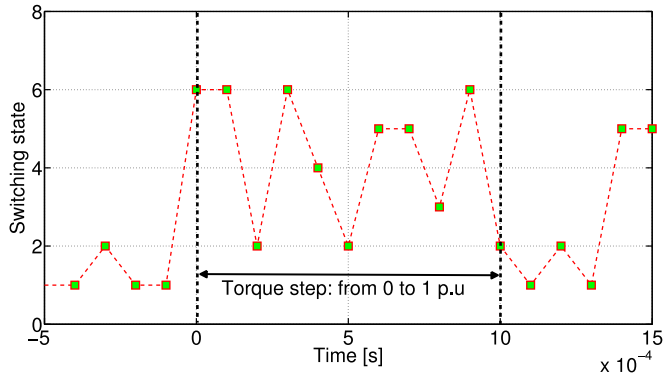

Fig. 14. Switching states torque step of the MPTC-LMC method (e.g., 1 represents zero voltage vector, 2–7 represent nonzero vectors).

method. This means that compared with the MPTC method, the MPTC-LMC strategy has almost the same steady-state performance, and considers the balance between inverter losses and machine losses.

B. Dynamic Performance

The transient response of the MPTC-LMC method is investigated in this section. One of the advantages of the MPTC method is the torque implementation of responding in time which through selecting only active voltage vectors. Thus, the selection of the voltage vectors of the MPTC-LMC method must be analyzed and verified. The torque step is from 0 to 2 N·m, which is generated by a speed step (from 0 to 2000 r/min). The switching states of the flexible voltage vectors produced by the two-level VSI are 000,...,111 . Both of 000 and 111 means the zero voltage vector. In the experiment, the switching states of the MPTC-LMC method are represented by seven Arabic numbers, e.g., Switching state $=$ 1 means 000,..., Switching state $=$ 7 means 110. The switching states of the MPTC-LMC method is shown in Fig. 14. It can be seen that during a torque step of the MPTC-LMC method, only the active voltage vectors are selected. In order to evaluate the dynamic control behavior, different speed reference steps have been applied to the system in this test. In Fig. 15, the speed reference is from 0 to 1000 r/min at 0 s. The measured electrical torque, the measured mechanical speed, and the stator current are investigated. It can be seen that the actual electrical torque can track the reference torque very well during both of the start-up processes; thus, the actual mechanical speed can also track the speed command very well. The robustness of the MPTC-LMC method is verified by a load torque disturbance experiment. The test IPMSM runs at 2000 r/min with a partial load. Two load steps (from 0.1 to 1 p.u., and from 1 to 0.1 p.u.) are applied to the control system at 1 and 3.2 s, respectively. The experimental result is shown in Fig. 16. It can be seen that the actual torque and speed can track the reference value over a torque disturbance.

C. Efficiency Optimization

Whether the system efficiency can be improved by flux adaptation or not, and how much is the loss minimized of the

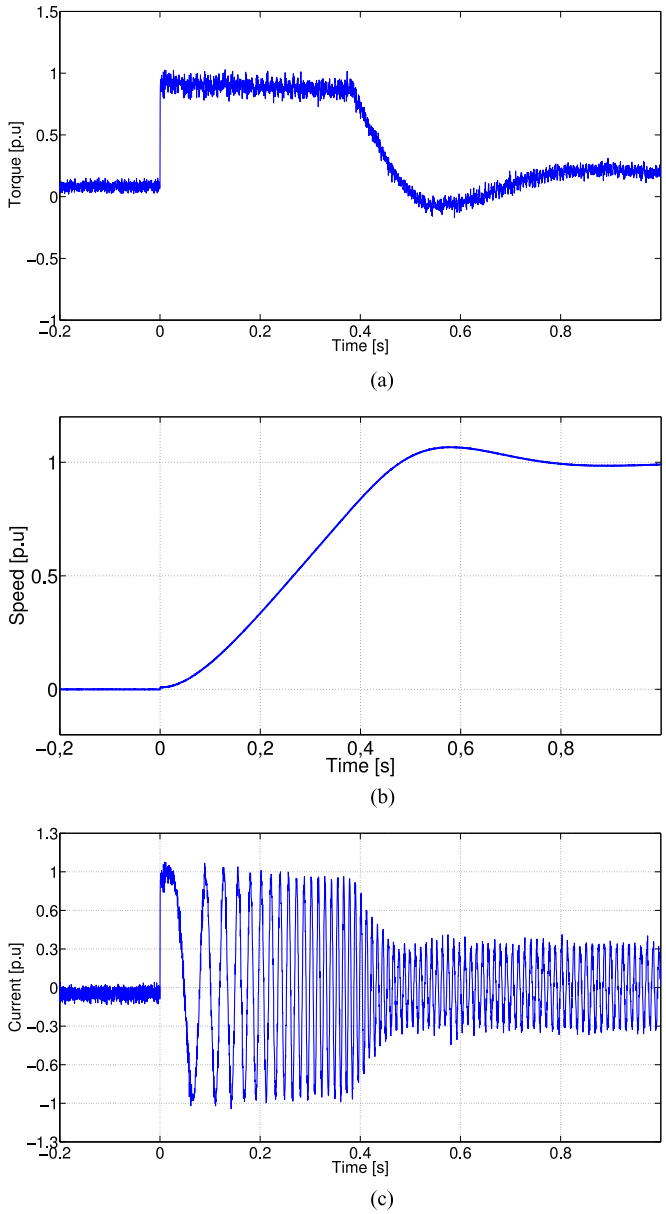

Fig. 15. Startup performance of the MTPC-LMC method. (a) Torque. (b) Speed. (c) Current.

MTPC-LMC method are the improvements compared to the conventional strategy. These are in large part dependent on the accuracy of the machine model and the measurements. Thus, in the experiments, the nonlinear machine parameters are applied through the lookup table. Furthermore, in order to improve the accuracy of the measurements, the influence of the temperature is also taken into account, i.e., a temperature sensor is used to monitor the temperature of the IPMSM, and an air cooling system is installed in the test bench. In the proposed MPTC-LMC method, the balance between machine losses and switching losses are considered by the cost function (23). Thus, in this section, both the machine and inverter losses of the MPTC-LMC method for the IPMSM are investigated and analyzed.

Fig. 17 shows the comparison of the switching state between the MPTC-LMC method and the MPTC strategy. It can be seen

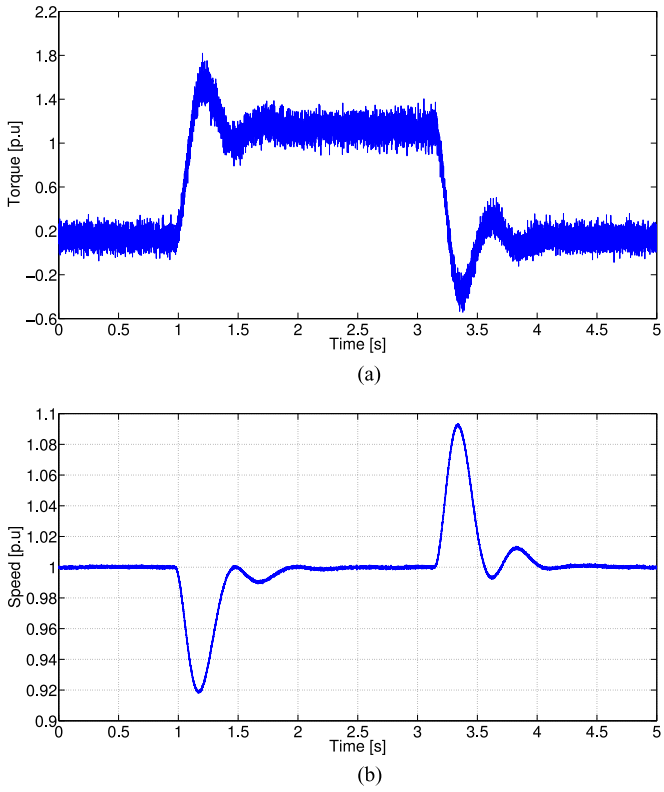

Fig. 16. Dynamic stiffness of the MPTC-LMC method. (a) Torque. (b) Speed.

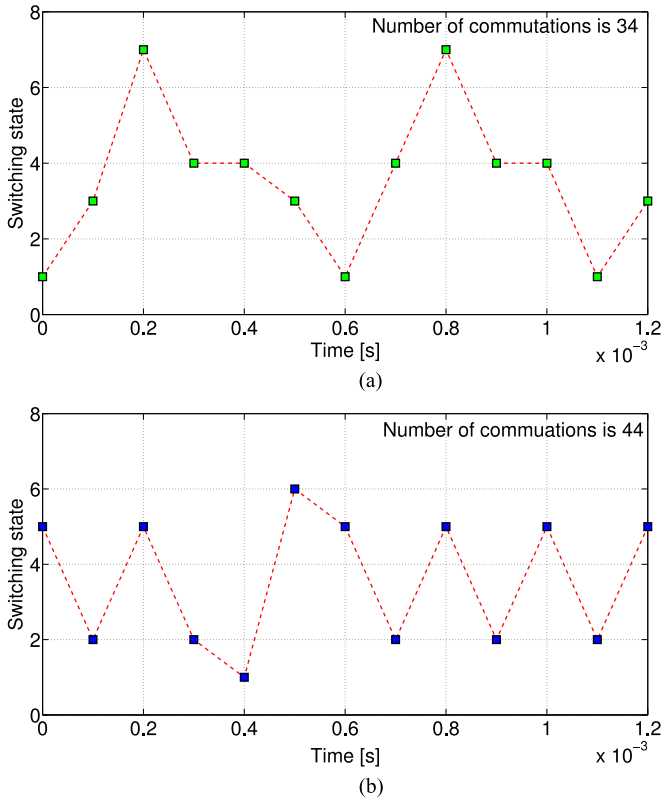

Fig. 17. Switching state. (a) MPTC-LMC method. (b) MPTC method.

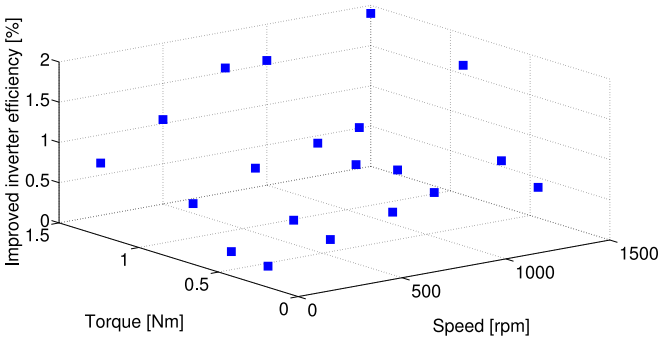

Fig. 18. Inverter efficiency improvement of the MPTC-LMC method.

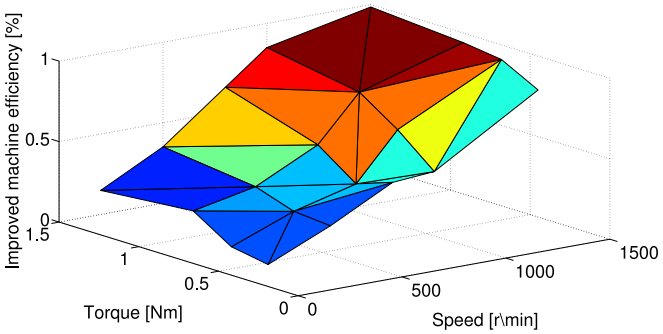

Fig. 19. Inverter efficiency improvement of MPTC with pure MTPA method.

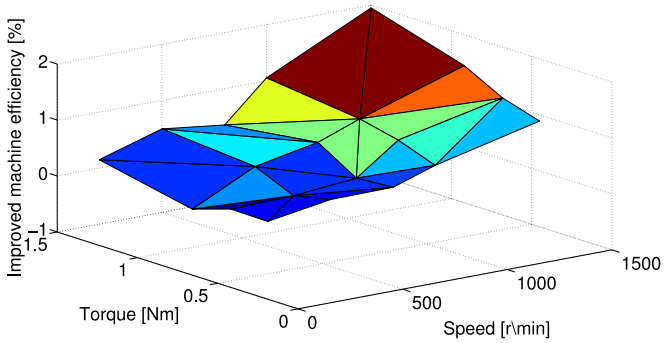

Fig. 20. Inverter efficiency improvement of MPTC with pure LMC method.

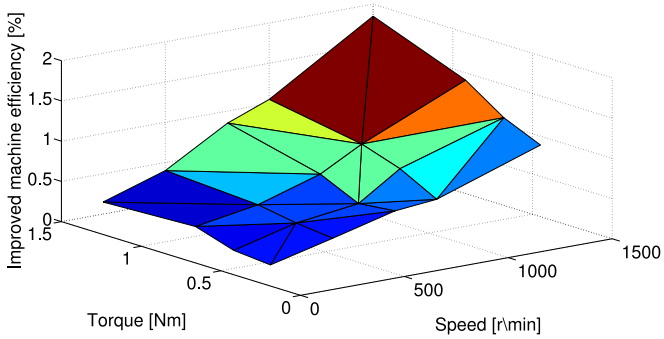

Fig. 21. Machine efficiency improvement of the MPTC-LMC method.

that the trajectories of the switching states of both methods are random. However, when taking the switching sequence or the switching loss into account, the total number of commutations of the power semiconductors (e.g., MOSFET) of the MTPC-LMC method is smaller than that of the MPTC method. The improvement of the inverter efficiency is shown in Fig. 18, which is achieved by balancing the inverter losses and control performance (e.g., torque and current). The proposed MPTC-LMC method takes the machine losses (e.g., copper loss, iron loss, and PM loss) into account by utilizing the alternative Gopinath-style LMC strategy. As preceding introduction, the Gopinath-style LMC method combines the pure LMC method and the MTPA method. In this section, compared with the conventional MPTC method, the machine efficiency improvement of MPTC with the pure MTPA method, the MPTC with the pure LMC method, and the MPTC-LMC MPTC strategy are compared and analyzed, respectively, as shown in Figs. 19–21. It can be seen that when the optimal strategies are integrated into the conventional MPTC method, the machine efficiency can be improved. By taking the iron loss and PM loss into account, the machine efficiency improvement of MPTC with the pure LMC method is higher than that of the MPTC with the pure MTPA method. However, due to the measurement errors of iron loss and PM loss, the calculated stator flux reference induces the efficiency decrease at relative low speed, as shown in Fig. 20. The proposed Gopinath-style LMC method can compensate the measurement error. As shown in Fig. 21, the improvement of machine efficiency of the MPTC-LMC method is obvious and without negative point.

VI. Conclusion

In this paper, the MPTC-LMC method has been proposed, developed, and implemented. This alternative solution of system efficiency optimization considers the machine losses and inverter losses simultaneously, and reduces the harsh requirement of the accuracy of the machine loss model. Furthermore, at relative low switching frequency discrete machine model is developed. The experimental steady-state performances, dynamic behaviors, inverter, and machine efficiency are investigated and analyzed in details.

The concept of the machine losses optimization strategy in this paper is based on a combination of the conventional MTPA method and the LMC method. In this paper, at the relative low-speed conditions, the copper loss of the machine is the dominate target to be optimized. The iron loss and PM loss will be considered gradually, when the percentage and measurement precision of the iron loss and PM loss rise with the increment of machine speed. This alternative solution can simplify the implementation of machine losses reduction and reduce the restrict accuracy requirement of total machine losses at relative low-speed conditions in practice. Compared with the pure LMC method, the proposed Gopinath-style LMC strategy shows a high tolerance of the flux trajectory. The performance has been evaluated by simulation and experimental results.

When using a FCS-MPTC with switching constraint, the switching sequence and the switching frequency can be optimized. It seems obvious that the inverter losses drop with the decreasing switching frequency. In order to compensate the drawback of the normal discrete machine model, which is

dependent on normal Euler function, an alternative discrete machine model based on improved Euler function is developed. It reduces the error of the predictive current at relative low switching frequency conditions. When comes to the motivation of system efficiency optimization, the machine losses and inverter losses are two key points. Thus, under an acceptable range of torque ripple, this paper finds a possible tradeoff point by balancing the system efficiency and drive properties (e.g., torque and current). In other words, the proposed solution exchanges appropriate drive performance for system efficiency. In this paper, the improvement of the system efficiency has been verified by experimental results.

In future work, in order to find a better balance point between system efficiency and control performance, an implementation of MPTC-LMC method under longer horizon prediction will be aimed. On the other hand, the switching frequency of medium large traction drive is constrained to a relative low value because of the high heat load caused by the high switching loss due to the high switching frequency, the proposed low switching frequency discrete machine model will be applied for power traction drive applications as medium large traction drive.

This proposed method provides an alternative solution for the system efficiency optimization, which can control the inverter losses and the machine losses by a cost function and the stator flux reference. The advantage of the strategy is that the two optimized targets (inverter losses and machine losses) are controlled separately. In a sense, compared with the efficiency optimization strategies based on only one parameter, this distributed strategy improves the reliability of the system, i.e., this increases the fault tolerance of the system.

Appendix A
Coefficients in (10)

The coefficients of optimal reference stator flux in (10) are shown as following:

$$a1 = (a+f)e^3 \tag{25}$$

$$b1 = be^3 + 3(a+f)bde^3 \tag{26}$$

$$y = -\frac{5}{6}B_1 + \frac{P}{3U} - U \tag{27}$$

$$B_1 = \frac{-3b1^2}{8a1^2} + \frac{c1}{a1} \tag{28}$$

$$B_2 = \frac{b1^3}{8a1^3} - \frac{b1c1}{2a1^2} + \frac{d1}{a1}. \tag{29}$$

The derivation of the coefficients in (10) are using the equations described as

$$a = \frac{3R_s}{L_d^2} \tag{30}$$

$$b = \frac{-3R_s\psi_{\mathrm{PM}}}{L_d^2} \tag{31}$$

$$c = \frac{4R_s}{3}\left(\frac{L_dT_e}{p}\right)^2 \tag{32}$$

$$d = L_q\psi_{\mathrm{PM}} \tag{33}$$

$$e = L_d - L_q \tag{34}$$

$$f = \frac{3\omega}{R_{Fe} + R_{\mathrm{PM}}} \tag{35}$$

$$g = \left(\frac{2L_dL_qT_e}{3p}\right)^2 \tag{36}$$

$$c1 = 3bde^2 + 3(a+f)d^2e \tag{37}$$

$$d1 = 3bd^2e + (a+f)d^3 \tag{38}$$

$$e1 = bd^3 - (ce + fge) \tag{39}$$

$$B_3 = \frac{-3b1^4}{256a1^4} + \frac{b1^2c1}{16a1^3} - \frac{b1d1}{4a1^2} + \frac{d1}{a1} \tag{40}$$

$$P = -\frac{B_1^2}{12} - B_3 \tag{41}$$

$$Q = -\frac{B_1^3}{108} + \frac{B_1B_3}{3} - \frac{B_2^2}{8} \tag{42}$$

$$U = \left|\sqrt[3]{\frac{Q}{2} \pm \sqrt{\frac{Q^2}{4} + \frac{P^3}{27}}}\right|. \tag{43}$$

Appendix B
Weighting Factor in (23)

Method:

Suppose that the different machine parameters have the same contribution to the cost function, and then the unitary method (44) is used to simplified the weighting factor. The simplified weighting factors of the cost function in (23) can be expressed as (45) and (46)

$$X_{\mathrm{p.u.}} = \frac{X - \min\{X_{i=1,2,\ldots,7}\}}{\max\{X_{i=1,2,\ldots,7}\} - \min\{X_{i=1,2,\ldots,7}\}} \tag{44}$$

$$Q_1 = \frac{\max\{T_{e,i=1,2,\ldots,7}\} - \min\{T_{e,i=1,2,\ldots,7}\}}{\max\{\Psi_{s,i=1,2,\ldots,7}\} - \min\{\Psi_{s,i=1,2,\ldots,7}\}} \tag{45}$$

$$Q_2 = \frac{\max\{T_{e,i=1,2,\ldots,7}\} - \min\{T_{e,i=1,2,\ldots,7}\}}{\max\{S_{i=1,2,\ldots,7}\} - \min\{S_{i=1,2,\ldots,7}\}}. \tag{46}$$

References

[1] R. Kennel, J. Rodriguez, J. Espinoza, and M. Trincado, "High performance speed control methods for electrical machines: An assessment," in *Proc. IEEE Int. Conf. Ind. Technol.*, Mar. 2010, pp. 1793–1799.

[2] P. Cortes, M. Kazmierkowski, R. Kennel, D. Quevedo, and J. Rodriguez, "Predictive control in power electronics and drives," *IEEE Trans. Ind. Electron.*, vol. 55, no. 12, pp. 4312–4324, Dec. 2008.

[3] M. Preindl and S. Bolognani, "Model predictive direct speed control with finite control set of PMSM drive systems," *IEEE Trans. Power Electron.*, vol. 28, no. 2, pp. 1007–1015, Feb. 2013.

[4] F. Wang, Z. Chen, P. Stolze, J.-F. Stumper, J. Rodriguez, and R. Kennel, "Encoderless finite-state predictive torque control for induction machine with a compensated MRAS," *IEEE Trans. Ind. Informat.*, vol. 10, no. 2, pp. 1097–1106, May 2014.

[5] S. Kouro, P. Cortes, R. Vargas, U. Ammann, and J. Rodriguez, "Model predictive control—A simple and powerful method to control power converters," *IEEE Trans. Ind. Electron.*, vol. 56, no. 6, pp. 1826–1838, Jun. 2009.

[6] R. Vargas, P. Cortes, U. Ammann, J. Rodriguez, and J. Pontt, "Predictive control of a three-phase neutral-point-clamped inverter," *IEEE Trans. Ind. Electron.*, vol. 54, no. 5, pp. 2697–2705, Oct. 2007.

[7] V. Yaramasu, M. Rivera, B. Wu, and J. Rodriguez, "Model predictive current control of two-level four-leg inverters—Part I: Concept, algorithm, and simulation analysis," *IEEE Trans. Power Electron.*, vol. 28, no. 7, pp. 3459–3468, Jul. 2013.
[8] M. Rivera, V. Yaramasu, J. Rodriguez, and B. Wu, "Model predictive current control of two-level four-leg inverters—Part II: Experimental implementation and validation," *IEEE Trans. Power Electron.*, vol. 28, no. 7, pp. 3469–3478, Jul. 2013.
[9] S. Kwak and J.-C. Park, "Switching strategy based on model predictive control of VSI to obtain high efficiency and balanced loss distribution," *IEEE Trans. Power Electron.*, vol. 29, no. 9, pp. 4551–4567, Sep. 2014.
[10] A. Bazzi and P. Krein, "Review of methods for real-time loss minimization in induction machines," *IEEE Trans. Ind. Appl.*, vol. 46, no. 6, pp. 2319–2328, Nov. 2010.
[11] G. Dajaku and D. Gerling, "A novel 12-teeth/10-poles PM machine with flux barriers in stator yoke," in *Proc. Int. Conf. Electr. Mach.*, Sep. 2012, pp. 36–40.
[12] X. Wang, W. Xie, G. Dajaku, R. Kennel, D. Gerling, and R. Lorenz, "Position self-sensing evaluation of novel CW-IPMSMs with a HF injection method," *IEEE Trans. Ind. Appl.*, vol. 50, no. 5, pp. 3325–3334, Sep. 2014.
[13] T. Jahns, G. Kliman, and T. W. Neumann, "Interior permanent-magnet synchronous motors for adjustable-speed drives," *IEEE Trans. Ind. Appl.*, vol. IA-22, no. 4, pp. 738–747, Jul. 1986.
[14] T. D. Do, S. Kwak, H. H. Choi, and J.-W. Jung, "Suboptimal control scheme design for interior permanent-magnet synchronous motors: An SDRE-based approach," *IEEE Trans. Power Electron.*, vol. 29, no. 6, pp. 3020–3031, Jun. 2014.
[15] S. Bolognani, L. Peretti, and M. Zigliotto, "Online MTPA control strategy for DTC synchronous-reluctance-motor drives," *IEEE Trans. Power Electron.*, vol. 26, no. 1, pp. 20–28, Jan. 2011.
[16] S. Morimoto, Y. Tong, Y. Takeda, and T. Hirasa, "Loss minimization control of permanent magnet synchronous motor drives," *IEEE Trans. Ind. Electron.*, vol. 41, no. 5, pp. 511–517, Oct. 1994.
[17] S. Morimoto, M. Sanada, and Y. Takeda, "Wide-speed operation of interior permanent magnet synchronous motors with high-performance current regulator," *IEEE Trans. Ind. Appl.*, vol. 30, no. 4, pp. 920–926, Jul. 1994.
[18] S. Vaez, V. John, and M. Rahman, "An on-line loss minimization controller for interior permanent magnet motor drives," *IEEE Trans. Energy Convers.*, vol. 14, no. 4, pp. 1435–1440, Dec. 1999.
[19] M. Uddin and S. W. Nam, "New online loss-minimization-based control of an induction motor drive," *IEEE Trans. Power Electron.*, vol. 23, no. 2, pp. 926–933, Mar. 2008.
[20] S. Vaez-Zadeh, "Torque compensation in permanent magnet synchronous motor drives for constant torque, varying flux operation," in *Proc. IEEE 31st Annu. Power Electron. Spec. Conf.*, Jun. 2000, vol. 3, pp. 1124–1129.
[21] J. Cleland, V. McCormick, and M. Turner, "Design of an efficiency optimization controller for inverter-fed ac induction motors," in *Proc. IEEE Ind. Appl. Conf. 30th IAS Annu. Meet.*, Oct. 1995, vol. 1, pp. 16–21.
[22] D. Graovac, M. Prschel, and A. Kiep, "MOSFET power losses calculation using the datasheet parameters," *Infineon, Neubiberg, Germany, tech. rep.*, 2006.
[23] M. Aguirre, P. Madina, J. Poza, A. Aranburu, and T. Nieva, "Analysis and comparison of PWM modulation methods in VSI-fed PMSM drive systems," in *Proc. Int. Conf. Electr. Mach.*, Sep. 2012, pp. 851–857.
[24] S. Kim, Y.-D. Yoon, S.-K. Sul, and K. Ide, "Maximum torque per ampere (MTPA) control of an IPM machine based on signal injection considering inductance saturation," *IEEE Trans. Power Electron.*, vol. 28, no. 1, pp. 488–497, Jan. 2013.
[25] C. Kral, T. Habetler, R. Harley, F. Pirker, G. Pascoli, H. Oberguggenberger, and C. J. M. Fenz, "Rotor temperature estimation of squirrel-cage induction motors by means of a combined scheme of parameter estimation and a thermal equivalent model," *IEEE Trans. Ind. Appl.*, vol. 40, no. 4, pp. 1049–1057, Jul. 2004.
[26] L. Alberti, E. Fornasiero, N. Bianchi, and S. Bolognani, "Rotor losses measurements in an axial flux permanent magnet machine," *IEEE Trans. Energy Convers.*, vol. 26, no. 2, pp. 639–645, Jun. 2011.
[27] J. S. Lee, C.-H. Choi, J.-K. Seok, and R. Lorenz, "Deadbeat-direct torque and flux control of interior permanent magnet synchronous machines with discrete time stator current and stator flux linkage observer," *IEEE Trans. Ind. Appl.*, vol. 47, no. 4, pp. 1749–1758, Jul. 2011.
[28] R. Lorenz, "The emerging role of dead-beat, direct torque and flux control in the future of induction machine drives," in *Proc. 11th Int. Conf. Optim. Electr. Electron. Equip.*, May 2008, pp. XIX–XXVII.
[29] P. Correa, J. Rodriguez, I. Lizama, and D. Andler, "A predictive control scheme for current-source rectifiers," *IEEE Trans. Ind. Electron.*, vol. 56, no. 5, pp. 1813–1815, May 2009.

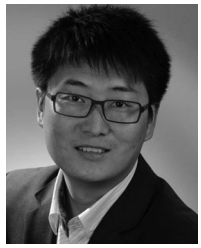

Wei Xie (S'13–M'14) was born in Inner Mongolia, China, in 1982. He received the B.S. and M.S. degrees in electrical engineering from Northwestern Polytechnic University, Xi'an, China, in 2007 and 2011, respectively. He is currently working toward the Doctorate degree at the University of Federal Defense Munich, Munich, Germany.

His research interests include advanced control for electrical drives and machine design.

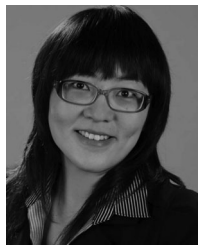

Xiaocan Wang (S'13–M'14) was born in Henan, China, in 1984. She received the B.S. and M.S. degrees in electrical engineering from Northwestern Polytechnic University, Xi'an, China, in 2007 and 2010, respectively. She is currently working toward the Doctorate degree at the Technical University of Munich, Munich, Germany.

Her research interest includes advanced control for electrical drives and power electronics.

Fengxiang Wang (S'13–M'14) was born in Jiujiang, China, in 1982. He received the B.S. degree in electronic engineering and the M.S. degree in automation from Nanchang Hangkong University, Nanchang, China, in 2005 and 2008, respectively. In 2014, he received the Ph.D. degree from the Institute for Electrical Drive Systems and Power Electronics, Technische Universitaet Muenchen, Munich, Germany.

He is currently working at Haixi Institutes, Chinese Academy of Sciences, Jinjiang, China. His research interests include predictive control and sensorless control for electrical drives.

Wei Xu (S'11–M'14) received the B.S. degree in mechanical engineering from Tongji University, Shanghai, China, in 2004, the M.S. degree in mechanical engineering from the Leibniz University of Hanover, Hanover, Germany, in 2007, and the Ph.D. degree from the University of Wisconsin, Madison, WI, USA, in 2013.

He is currently working at Ford Motor Company as a Motor Control Engineer, Dearborn, MI, USA. His research interests include electrical machines and drive control.

Ralph Kennel (M'89–SM'96) was born in 1955 at Kaiserslautern, Germany. He received the Diploma and Dr.-Ing. (Ph.D.) degrees from the University of Kaiserslautern, Kaiserslautern, in 1979 and 1984, respectively.

From 1994 to 1999, he was appointed as a Visiting Professor at the University of Newcastle-upon-Tyne, England, U.K. From 1999 to 2008, he was a Professor for electrical machines and drives, Wuppertal University, Germany. Since 2008, he has been a Professor for electrical drive systems and power electronics, Technische Universtaet Muenchen, Munich, Germany. His main research interests include sensorless control of ac drives, predictive control of power electronics, and hardware-in-the-loop systems.

Dr. Kennel is a Fellow of the Institute of Electrical Engineering and a Chartered Engineer in the U.K. Within IEEE, he is a Treasurer of the Germany Section as well as the ECCE Global Partnership Chair of the Power Electronics Society.

Dieter Gerling (M'01) was born in 1961. He received the Diploma and Ph.D. degrees in electrical engineering from the Technical University of Aachen, Aachen, Germany, in 1986 and 1992, respectively.

From 1986 to 1999, he was with Philips Research Laboratories, Aachen, as a Research Scientist and later as a Senior Scientist. In 1999, he joined Robert Bosch GmbH, Buehl, Germany, as the Director. Since 2001, he has been a Full Professor at the University of Federal Defense Munich, Munich, Germany. He is the Head of the Institute of Electrical Drives, University of Federal Defense Munich.